

Feudal Networks for Visual Navigation

Faith Johnson

Rutgers University
faith.johnson@rutgers.edu

Bryan Bo Cao

Stony Brook University
boccao@cs.stonybrook.edu

Kristin Dana

Rutgers University
kristin.dana@rutgers.edu

Shubham Jain

Stony Brook University
jain@cs.stonybrook.edu

Ashwin Ashok

Georgia State University
aashok@gsu.edu

Abstract—Visual navigation follows the intuition that humans can navigate without detailed maps. A common approach is interactive exploration while building a topological graph with images at nodes that can be used for planning. Recent variations learn from passive videos and can navigate using complex social and semantic cues. However, a significant number of training videos are needed, large graphs are utilized, and scenes are not unseen since odometry is utilized. We introduce a new approach to visual navigation using feudal learning, which employs a hierarchical structure consisting of a worker agent, a mid-level manager, and a high-level manager. Key to the feudal learning paradigm, agents at each level see a different aspect of the task and operate at different spatial and temporal scales. Two unique modules are developed in this framework. For the high-level manager, we learn a *memory proxy map* in a self supervised manner to record prior observations in a learned latent space and avoid the use of graphs and odometry. For the mid-level manager, we develop a *waypoint network* that outputs intermediate subgoals imitating human waypoint selection during local navigation. This waypoint network is pre-trained using a new, small set of teleoperation videos that we make publicly available, with training environments different from testing environments. The resulting feudal navigation network achieves near SOTA performance, while providing a novel no-RL, no-graph, no-odometry, no-metric map approach to the image goal navigation task.

I. INTRODUCTION

Visual navigation is motivated by the idea that humans likely navigate without ever building detailed 3D maps of their environment. In psychology, the concept of cognitive maps and graphs [1–4] formalizes this intuition, and experiments have shown the potential validity of the idea that humans build approximate graphs of their environment encoding relative distances between landmarks. In vision and robotics, these ideas have translated to the construction of topological graphs and maps based solely on visual observations. Visual navigation paradigms seek new representations of environments that are rich with semantic information, easy to dynamically update, and can be constructed faster and more compactly than full 3D metric maps [5–9].

Reinforcement Learning (RL) is often used for navigation in known environments and has clear success in training games where the reward is well-defined [10–12]. Distance-to-goal has become a reward proxy in many recent works that use an RL framework for navigation [13, 14]. We take inspiration from Feudal RL [15] to craft our visual navigation framework. Feudal RL decomposes a task into sub components and can provide significant advantages for both training and performance that we find particularly well-suited for the task of visual navigation. The feudal framework identifies *workers*

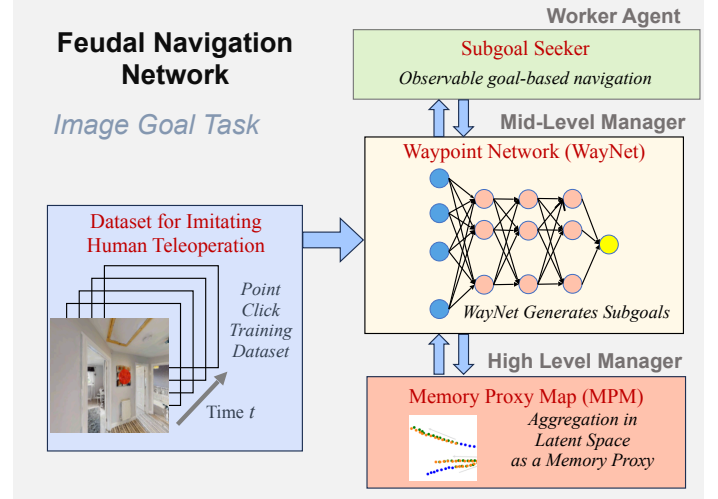


Fig. 1. Feudal Navigation Network (FeudalNav), providing a no-RL, no-odometry, no-graph, and no-metric map visual navigation agent for the image-goal task on previously unseen environments. The three main components are: (1) a high level manager that creates a memory proxy map (MPM) to use as an aggregate observation to make high-level navigation decisions, (2) a mid-level manager waypoint network (WayNet) that mimics human teleoperation by predicting visible points in the environment to guide worker agent exploration, and (3) a low level worker that finds the subgoal using robust point matching.

and *managers*, and allows for multiple levels of hierarchy (ie. mid-level and high-level managers). Each of these entities observes different aspects of the task *and* operates at a different temporal or spatial scale. For navigation in unseen environments, this dichotomy is ideal to make the overall task more manageable. The worker-agent can focus on local motion, but manager-agents can direct navigation and assess when it is time to move to new regions.

However, in this work we focus on visual navigation with no odometry and in unknown environments, so distance-based reward is not readily available to train an RL agent. Recent work called NRNS [16], which builds a topological graph using both images and odometry information, has challenged the need for RL and instead uses a distance estimator by training with passive videos. Inspired by NRNS, we also use “no-RL” so that no policy is learned via reinforcement/interaction with an environment. We take advantage of the feudal RL network structure and show its benefits under supervised and self-supervised no-RL learning paradigms. Our approach uses no metric maps, no graphs, and no odometry information, resulting in a lightweight easy-to-train framework that still has high/SOTA performance in image-goal navigation tasks.

Key to our approach is representing the traversed environment with a learned latent map (instead of a graph) that acts as a memory proxy during navigation. This *memory proxy map (MPM)* is obtained using self-supervised training. The high-level manager maintains the MPM as the agent navigates in novel environments and polls its density to determine when a region is well-explored and movement away from the current region is desired. A second key aspect to our approach is a *waypoint network (WayNet)* for the middle-level manager which outputs visible sub-goals for the worker agent to move towards. We train WayNet to imitate human teleoperation and collect a dataset with a human teleoperator tasked with point click navigation through a set of Gibson environments [17] in Habitat AI [18] (a simulation environment comprised of scans of real scenes). The resulting “image and point-click” pairs are used to train WayNet in a set of environments different from the image-goal testing environments. The intuition is that when humans navigate a simulated environment using point-click teleoperation, they use a skill of choosing a single point in the observation to move toward. For example, the chosen point may be toward the end of a hallway, toward a door, or further into a room. We demonstrate that this skill is easily learnable and generalizes to new environments with zero-shot transfer. Our dataset of images and point-clicks is made publicly available with this paper.

Our contributions are fivefold:

- 1) Hierarchical navigation framework (FeudalNav) using agents operating at different spatial and temporal scales
- 2) A lean, no-graph navigation approach using a self-supervised memory proxy map (MPM)
- 3) WayNet, a waypoint network for learned local navigation
- 4) A dataset ¹ of 103K point-clicks from human teleoperation in multiple environments made publicly available and useful for training a waypoint network
- 5) SOTA performance on the image-goal task in Habitat indoor environments (testing and training on distinct environments)

II. RELATED WORK

A. Visual Navigation

Visual navigation aims to build representations that incorporate the rich information of scene images, interjecting image-based learning in traditional mapping/planning navigation frameworks [13, 20–23]. Visual navigation methods can be categorized based on how environments are represented. Early work focused on creating full metric maps of a space using SLAM augmented by images [6, 21]. While full metric maps can be ideal, especially if the space can be mapped before planning, the representations are computationally complex. Topological graphs and maps can lighten this load and provide image data at nodes and relative distances at edges [5, 24]. While easier to build, these methods have the potential for large memory requirements, especially if new nodes are

added every time an agent takes an action in the environment [13, 25, 26].

One solution to this problem is sparser topological graphs [16, 27] that retain information useful for navigation. Visual features of unexplored next-nodes are sometimes predicted or hallucinated [16, 26]. Some methods go a step further by pairing semantic labels with the graph representation [28]. However, these methods break down in environments that are sparsely furnished, have many duplicate objects, or contain uncommon objects that may not appear in popular object detection datasets. Another solution is to only use graphs during training to build 2D embedding space representations of environments, i.e. potential fields or functions, that preserve important physical [29, 30], visual [31], or semantic [32–34] relationships between regions in the environment. Our work more closely aligns with this line of work, but we do not use any graph networks or inference and instead build our 2D latent map, the memory proxy map, using self-supervision. Additionally, unlike many of the methods above, we do not require the agent to have information about the test environment before deployment, use reinforcement learning, or learn metric maps.

B. Feudal Learning

Feudal learning originated as a reinforcement learning (RL) framework [15, 35]. Researchers have explored RL for the image-goal visual navigation task [36], most notably using external memory buffers [37–40]. However, it still suffers from several issues such as sample inefficiency, handling sparse rewards, and the long horizon problem [41, 42]. Feudal reinforcement learning, characterized by its composition of multiple, sequentially stacked agents working in parallel, arose to combat these issues using temporal or spatial abstraction, mostly in simulated environments [15] where its effects can be more easily compared to other methods. Some of these task hierarchies are hand defined [43], while others are discovered dynamically with [44] or without [45] human input.

The feudal network paradigm has been adopted by other learning schemas outside of RL in recent years. In navigation, hierarchical networks are commonly used to propose waypoints as subgoals during navigation [46], typically working in a top-down view of the environment [47] with only two levels of agents [48]. Our work uses multiple agent levels, operates in the first person point of view for predicting waypoints, and reaps the benefits of this feudal relationship without using reinforcement learning.

III. HUMAN NAVIGATION DATASET

Humans are already adept navigators, but teaching agents to learn proficient navigation policies often requires distilling complex concepts and strategies into mathematical equations to be used for reward or loss functions. However, it is possible to avoid this lengthy process by implicitly learning policies directly from observations of human behavior. We collect videos of human driven trajectories through multiple simulated and real world environments to be used for this purpose.

¹Dataset can be accessed here: <https://zenodo.org/records/10608067>. DOI: 10.5281/zenodo.10608067.



Fig. 2. Samples of RGB images in our human navigation dataset captured from an ego-centric camera in both Gibson [17] and Matterport [19] environments. Video frames start from left to right. A human provides point-click guidance for robot visual navigation visualized with red dots.

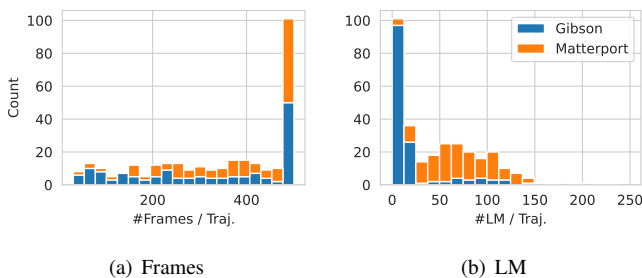


Fig. 3. Stacked histograms depicting #Frames and #LM per trajectory. (a) the majority of trajectories consists of the maximum #Frames 500. The number of human point-click waypoints is equal to the number of frames for each scene. (b) most trajectories in the Gibson rooms consists of only a small number of annotated landmarks (e.g. < 25), while it increases in Matterport due to its larger and more complicated environments. (LM denotes landmark.)

	#Traj.	#LM	Tot. #Frames	#Frames / Traj.
G	150	3,744	48,130	321
MP	150	10,537	55,368	369
All	300	14,281	103,498	345

TABLE I
STATISTICS OF OUR HUMAN NAVIGATION DATASET. WE DETAIL THE NUMBER OF TRAJECTORIES, LANDMARK ANNOTATIONS, TOTAL NUMBER OF FRAMES AND AVERAGE NUMBER OF FRAMES PER TRAJECTORY. EACH TRAJECTORY IS RECORDED IN A DISTINCT ENVIRONMENT. LM: LANDMARKS, G: GIBSON, MP: MATTERPORT.

A. Environments

We provide human point-click waypoint and landmark annotations during navigation for a selection of the Gibson [17] and Matterport [19] environments in Habitat-Sim [18, 49] to facilitate virtual environment exploration, as shown in Figure 2. Habitat is already used to train many visual navigation methods, so having in-domain, landmark-aware data will allow for direct extensions of these methods for greater ease of model comparison. Additionally, collecting data in simulation allows for greater collection volume and lower data processing time.

B. Data Collection and Representation

Instead of having agents reason over low level motor actions, we leverage the simulator to enable reasoning over high

level actions, like “turn left”, “turn right”, and “go forward”. These simplified actions also allow for a simplification of the human feedback needed to collect this trajectory data. To start, the human navigator is placed at a random, navigable point in an environment, and tasked with visiting as many rooms as possible while identifying distinct waypoints in each room. The current first person observation of the environment is shown on a screen, and the human moves through the environment by left clicking on this image in the direction they would like to move. There are three discrete action choices for moving around in the environment: moving forward 0.25m, turning left 15° , and turning right 15° . We map each human point click to a combination of these three actions as specified in Figure 5, execute them in the environment, then give the human the resulting new frame to continue the navigation process. To specify a landmark (or useful point for localization), the navigator right clicks on the observation image over the object or region of space they choose.

We record the sequence of observations (RGBD images), actions, navigation point clicks, and environment locations (X,Y,Z coordinates) as the navigator moves through each space. A list of pairs of point-click coordinates and their corresponding image observations is also provided so that landmarks may be easily identified in the scenes. Each human-guided trajectory is terminated after 500 actions or when the annotator has navigated through the entirety of the space, whichever comes first. We summarize the data distribution in Figure 3 and dataset statistics in Table I.

IV. METHODS

We start with an overview of our feudal navigation agent (FeudalNav), which is split into three levels, in Figure 4. First, we collect human navigation point-click supervision trajectories from several simulated environments as detailed in Section III. Then, we find clusters in that data corresponding to each unique visual area. The high level manager network learns a latent space in a self-supervised manner that serves as an approximate distance preserving memory module (memory proxy map) for navigation from this clustered data. The mid-level manager network (waypoint network) uses this memory

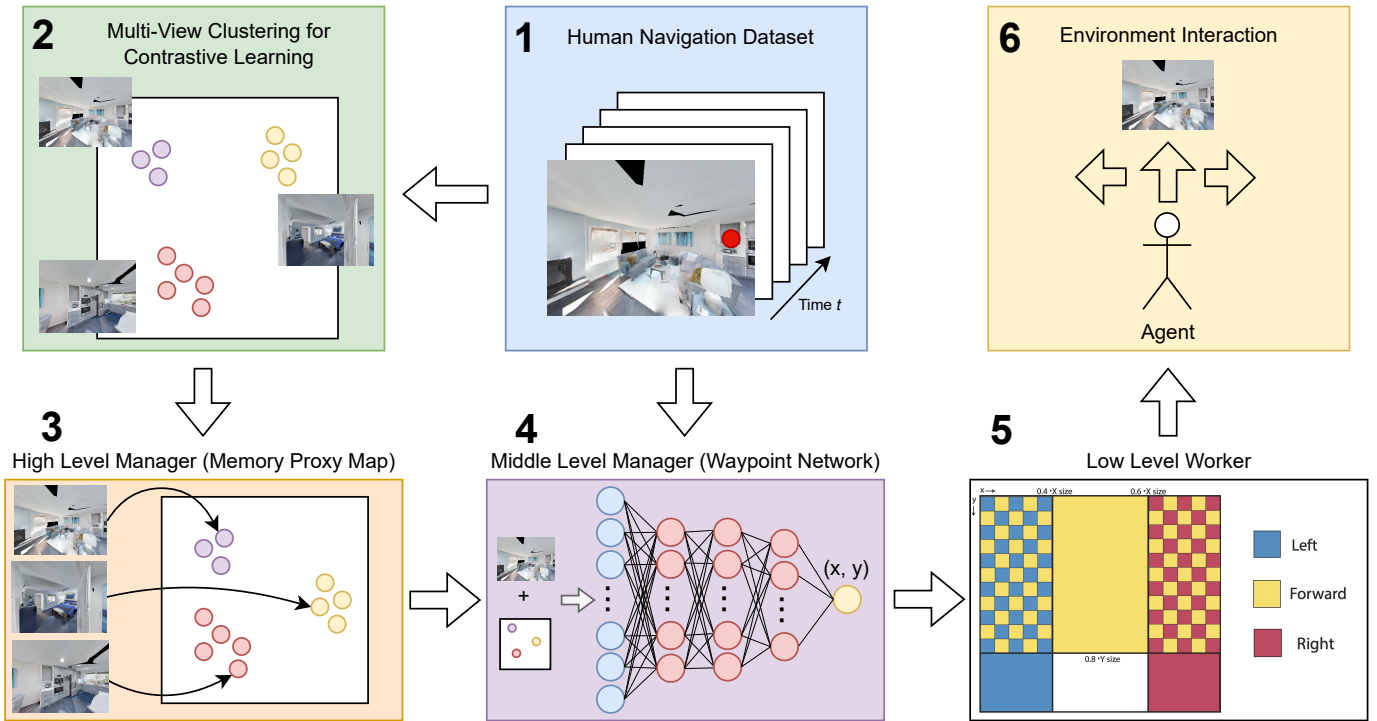


Fig. 4. **1:** Point click data is collected while human teleoperators direct agent exploration of different environments. The resulting set of point-image pairs comprise the human navigation dataset. **2:** From this dataset, we find clusters of observations based on feature similarity. **3:** These clusters are used to provide positive pairs to train the navigation memory module that serves as the high level manager (HLM) for our navigation agent. During test time, this HLM creates a map of historical agent locations (memory proxy map) in the learned space. **4:** These maps are created for the human navigation dataset and used to train the mid-level manager. During training, the memory proxy map and the current observations are used to predict human-like point click supervision to guide environment exploration. **5:** Based on this point click guidance, the worker executes low level actions directly in the simulated environment. (See Figure 5) **6:** During test time, these low level actions guide agent movement and produce new observations as input for the upper levels of the hierarchy.

representation and the current observation to mimic human navigation policies by predicting a point in the environment to move towards. The low level worker agent uses this predicted point to choose which actions to execute in the environment. We also add several goal-directed modules to our architecture that utilize Superglue [50] in order to test FeudalNav on the image-goal navigation task.

A. High-Level Manager: Memory

We contrastively learn a latent space that preserves an approximate distance between images to be used to build an aggregate memory proxy map (MPM). We learn this self-supervised latent space using a modified implementation of SMoG [51] that combines instance level contrastive learning and clustering methods. We choose this model because its momentum grouping gives it the capability of conducting both instance and group level contrastive learning simultaneously, which allows it to avoid the pitfall of other contrastive methods of using false negative pairs. We add further modifications to model training in order to conduct navigation-aware, self-supervised contrastive learning.

Instead of using typical augmentation methods during training, we rely on the slight variations introduced through multiple real world views to learn robust image representations. To determine positive pairs, we dynamically build clusters of images in the environment based on visual similarity. To

do this, we choose representative images to serve as cluster centers for each room or distinct environment area during navigation. As an agent traverses through an environment, the current observation is compared to the memory bank of previously seen cluster centers using Superglue [50], a feature matching method for robust keypoint matching. If the feature matching confidence provided by Superglue is above a threshold ψ , it is added to the corresponding cluster with the highest confidence score. If it is below that threshold, it is added as a new cluster center. We build these clusters per environment for all training trajectories and randomly sample positive pairs from each cluster to train the network.

During inference, we sequentially place observation images in this latent space to dynamically build a memory proxy map of previously visited locations. We find clusters in this latent space in a similar way as during training, but using the contrastively learned image features instead of utilizing the Superglue network. If the mean squared error (MSE) between the learned features of any of the existing cluster centers C_f and the features I_f^t from the new observation at time t is below a threshold α , it is considered to be part of the cluster with the lowest MSE. That is, if $MSE(C_f, I_f^t) < \alpha$ it is added to the cluster with the lowest MSE. However, if $MSE(C_f, I_f^t) > \alpha$, it is added as a new cluster center.

To update the MPM, we use the isomap algorithm to project each discovered cluster center from the image feature space

to a 2-D latent space that preserves the distance between the learned features. Then, a region around each projected cluster center in the 2D map is incremented and the radius of the region indicates the number of historical observations assigned to each cluster. This process yields a map with circular regions of varying sizes corresponding to how much exploration has occurred around each location. By representing the map with three channels, analogous to RGB, the increments are made with 3-channel values designating a unique “color” to each cluster center in order to help localize the agent. The more a room in an environment is explored, the larger the region in the MPM corresponding to this area. Looking at this coded cluster density gives the network an idea of how much exploration is left to do in a given space and signals when it is time to move to a new area using the relative image feature distance between the current observation and representative samples of previously seen areas, without the need for metric maps or SLAM. The approach is an approximate memory proxy, that is demonstrably effective and efficient for the image-goal navigation task.

B. Mid-Level Manager: Direction

For this module, we leverage human knowledge to learn optimal navigation policies directly from demonstrations collected in our human navigation dataset without the use of RL. Using the current RGBD observation and the memory proxy map from the high level manager as input, we finetune Resnet-18 [52] to predict the pixel coordinate directing the navigation agent’s motion in the environment. We alter the first layer of Resnet so that it can accept a seven channel input and concatenate the RGBD observation and the (RGB) memory proxy map together along the channel dimension to use as input. We also create a second version of the mid-level manager that takes in multiple of these RGBD-Map compound inputs in order to give the network more context about recently visited areas. For this network version, which we use in Stacked FeudalNav, we use the RGBD-Map input of the previous two frames and the current observation concatenated together along the channel dimension as input to WayNet to predict the next navigation waypoint.

The key intuition here is that the high level manager reasons about the navigation task at a more global view and coarser grained spatial scale than the mid-level manager, that has a first person, more fine-grained view of the environment. Breaking the problem into these two spatial scales introduces spatial abstraction which allows these two networks to work in tandem to solve smaller pieces of the overall problem. Stacked FeudalNav’s input that covers three time steps further introduces a level of temporal abstraction between the high level manager, which now operates at a coarser grained time scale, and the mid level manager, which has a more fine grained time scale, which further breaks down the original navigation task. These simplifications allow for faster training with smaller amounts of data.

To enable goal-directed navigation, we again utilize the Superglue [50] network for keypoint matching. For each new

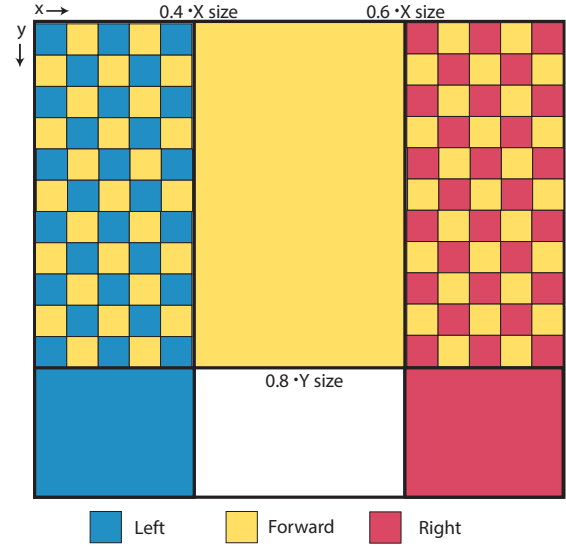


Fig. 5. Map showing mid-level manager point click locations map to which simulator actions for the low level worker. The bottom left grid (blue) and the bottom right grid (red) correspond to “turn left” and “turn right” respectively. The center middle grid (yellow) corresponds to “move forward”. The top left grid (blue and yellow) and the top right grid (red and yellow) correspond to the joint action of turning (left for blue and right for red) and moving forward sequentially. The two vertical delineations are at 0.4 and 0.6 times the x dimension of the observation respectively. The horizontal line is drawn at 0.8 times the y dimension of the observation.

observation, the network predicts a waypoint for exploration. Concurrently, Superglue computes keypoint matches between the current observation and a goal image. If the confidence of this keypoint match is above a threshold β , the average of the matched keypoints is used in the navigation pipeline instead of the waypoint prediction. If this is not the case, then the originally predicted exploration waypoint is used instead.

C. Low-Level Worker: Action

The low level worker agent takes actions in the environment based on the waypoint predicted by the mid-level manager. We define three environment level actions: “turn left by 15 degrees”, “turn right by 15 degrees”, and “move forward by 0.25 meters (m)”. The observation is split into a grid with three columns and two rows, shown in Figure 5, and the location of the predicted point determines which actions are taken. The bottom left (blue) and bottom right (red) grids correspond to “turn left” and “turn right” respectively. The top middle section (yellow) corresponds to “move forward”. The top left (blue and yellow) and top right (red and yellow) grids correspond to the action sequence of first turning (left or right respectively) and then moving forward. Predicting a waypoint in the bottom middle white box results in no action being taken. The agent chooses to stop when the Superglue [50] confidence threshold for matching goal image features to the current observation is above the threshold β and the depth measurement from the RGBD observation indicates that the middle of the matched keypoints has a depth less than or equal to 1m.

We introduce temporal abstraction into the relationship between the mid-level manager and the low level worker by enforcing that the two networks will operate at different temporal

scales. The worker makes t actions in the environment for each exploration waypoint provided by the mid-level manager. For the first of these t actions, it directly uses the predicted waypoint as its supervisory signal. We take a crop around the waypoint in the original observation and use Superglue [50] to match it to a location in the new observations for the remaining $t - 1$ actions. The average of the keypoint matches is used as the waypoint to determine the new actions for each successive time step. We also add a level of stochasticity to the worker agent. With probability ϵ , it takes random actions in the environment that do not necessarily correspond to the waypoint supervision from the mid-level manager in order to further promote exploration.

V. EXPERIMENTS

A. Image-Goal Navigation Task

We test the performance of FeudalNav on the image-goal task. To start, the agent is placed in a previously unseen environment and given an RGBD image observation of the first person view of their surroundings. It is also given a goal image (RGB) of an object or region in the scene to find. All images are 480×640 pixels with 120° field of view. A trial terminates if the agent is able to get within 1m of the location of the goal image or the agent takes 500 actions in the environment. We define three environment level actions: “turn left 15° ”, “turn right 15° ”, and “move forward 0.25m” for the agent to choose from. The combined action choice of turn+forward represented by the upper left and right quadrants in Figure 5 counts as two actions towards the agent action limit. Each agent trajectory is evaluated on success rate, which measures whether or not the agent has reached the goal, and SPL, which is a measure of success weighted by inverse path length.

$$SPL = \frac{1}{N} \sum_{i=0}^N S_i \frac{l_i}{\max(l_i, p_i)}$$

where N is the total number of trajectories considered, S_i is an indicator variable for success, l_i is the optimal (shortest) geodesic path length between the starting location and the goal, and p_i is the actual path length the agent traveled.

B. Training Procedure

We train our networks using the human navigation dataset detailed in Section III. We use a subset of 117 trajectories with a total of 36834 frames. For the Superglue [50] confidence threshold when creating the clusters from the human navigation dataset or matching goal image features to the current observation, we choose $\psi = \beta = 0.7$. We choose $\alpha = 300$ for the threshold for assigning a learned image feature from SMOG [51] to an existing cluster center of the memory proxy map. The mid-level manager and the low level worker operate at different time scales, so the worker takes $t = 2$ steps in the environment for every one manager waypoint. Additionally, the worker takes random actions in the environment with a probability of $\epsilon = 0.1$.



Fig. 6. (Best viewed zoomed) We show qualitative results for the waypoints predicted by WayNet (blue) juxtaposed with the ground truth human click points from the human navigation dataset (orange). Note that the majority of the samples show high overlap between the two. When they diverge, the WayNet waypoints still lead to navigably feasible areas in each observation.

C. Testing Procedures

We test FeudalNav using the testing procedure and baselines outlined in NRNS [16]. Testing trajectories come from a publicly available set of Gibson [17] environments listed in [16]. They consist of approximately $6k$ point pairs (start and goal locations) that are uniformly sampled from fourteen environments and divided equally across the following categories. Straight trajectories involve two points where the ratio between the shortest geodesic distance and the euclidean distance between the points is less than 1.2 and the difference between the ground truth start and stop orientations is less than 45° . Curved trajectories involve point pairs where either of these conditions cannot be satisfied. Easy trajectories involve points that are $[1.5 - 3m]$ apart, medium trajectories have endpoints that are $[3 - 5m]$ apart, and hard trajectories have endpoints that are $[5 - 10m]$ apart by euclidean distance.

We compare our method performance using a flat RL DD-PPO [53] trained for varying lengths of time directly in the simulator, behavior cloning (BC) with a resnet-18 backbone and either a GRU or a metric map from [16], as well as with NRNS itself [16]. We believe this is the best baseline for our method due to the fact that they train from passive videos, use a (relatively) low amount of training data compared to other SOTA, minimally use graphs, and do not train in simulation. There are other recent works that test on the image-goal task that we believe are an unfair comparison with our work due to their use of methods (scene reconstruction [54], transfer learning [34], long training times ie. 53 GPU days [55], panoramic image input [28]) that are outside the scope of this paper due to their computationally heavy nature and/or requiring testing in previously seen environments.

Path Type	Model	Easy		Medium		Hard		Average	
		Succ \uparrow	SPL \uparrow	Succ \uparrow	SPL \uparrow	Succ \uparrow	SPL \uparrow	Succ \uparrow	SPL \uparrow
Straight	RL (10M steps) * [53]	10.50	6.70	18.10	16.17	11.79	10.85	13.46	11.24
	RL (extra data + 50M steps) * [53]	36.30	34.93	35.70	33.98	5.94	6.33	25.98	25.08
	RL (extra data+100M steps) * [53]	43.20	38.54	36.40	34.89	7.44	7.20	29.01	26.88
	BC w/ ResNet + Metric Map [16]	24.80	23.94	11.50	11.28	1.36	1.26	12.55	12.16
	BC w/ ResNet + GRU [16]	34.90	33.43	17.60	17.05	6.08	5.93	19.53	18.80
	NRNS w/ noise [16]	64.10	55.43	47.90	39.54	25.19	18.09	45.73	37.69
	NRNS w/out noise [16]	68.00	61.62	49.10	44.56	23.82	18.28	46.97	41.49
	FeudalNav (Ours)	61.40	51.81	50.30	40.10	31.02	23.33	47.57	38.41
Curved	Stacked FeudalNav (Ours)	65.90	48.50	51.00	29.22	33.62	14.49	50.17	30.74
	RL (10M steps) * [53]	7.90	3.27	9.50	7.11	5.50	4.72	7.63	5.03
	RL (extra data + 50M steps)* [53]	18.10	15.42	16.30	14.46	2.60	2.23	12.33	10.70
	RL (extra data+100M steps)* [53]	22.20	16.51	20.70	18.52	4.20	3.71	15.70	12.91
	BC w/ ResNet + Metric Map [16]	3.10	2.53	0.80	0.71	0.20	0.16	1.37	1.13
	BC w/ ResNet + GRU [16]	3.60	2.86	1.10	0.91	0.50	0.36	1.73	1.38
	NRNS w/ noise [16]	27.30	10.55	23.10	10.35	10.50	5.61	20.30	8.84
	NRNS w/out noise [16]	35.50	18.38	23.90	12.08	12.50	6.84	23.97	12.43
	FeudalNav (Ours)	41.30	19.51	32.60	17.10	18.60	10.88	30.83	15.83
	Stacked FeudalNav (Ours)	56.40	21.37	44.10	17.41	21.00	7.30	40.50	15.36

TABLE II

QUANTITATIVE COMPARISON OF OUR METHOD (FEUDALNAV AND STACKED FEUDALNAV) AGAINST BASELINES AND SOTA ON THE IMAGE GOAL TASK FOLLOWING THE EVALUATION PROTOCOL FROM NRNS [16] IN PREVIOUSLY UNSEEN GIBSON ENVIRONMENTS [17]. THE TOP RESULTS ARE BOLD FOR EACH CATEGORY. WE SHOW A 69% AND 27% INCREASE IN PERFORMANCE (SUCCESS RATE AND SPL RESPECTIVELY) ON CURVED TRAJECTORIES ON AVERAGE OVER NRNS, AND A 7% INCREASE IN PERFORMANCE ON THE STRAIGHT SUCCESS RATE. (* DENOTES THE USE OF A SIMULATOR.)

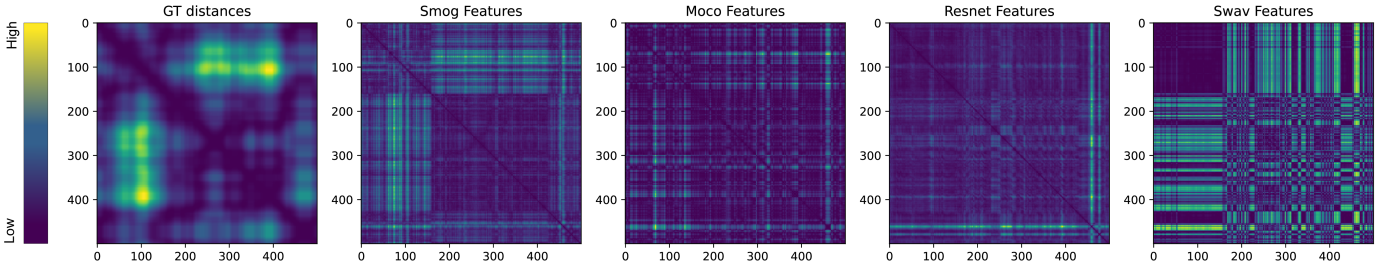


Fig. 7. We compare feature distances between all pairs of images in an example trajectory from the human navigation dataset for different self-supervised contrastive learning methods against the ground truth distances for each pair of images. Lower feature distances are darker/purple and higher feature distances are brighter/yellow. We show that SMOG [51] learns a latent space that preserves ground truth distance trends the most, making it the most suitable for the memory proxy map.

VI. RESULTS

A. Mid-Level Manager Accurately Mimics Human Navigation

Figure 6 shows qualitative examples of the mid-level manager’s predicted waypoints (blue) juxtaposed with the human ground truth point clicks (orange). For the majority of the points, both the predictions and the ground truth lie in the same area of the same object. When this is not true, the mid-level manager’s predicted waypoints still lead to feasibly navigable areas such as other doorways or further into rooms, thus showing that they mimic human navigation.

B. FeudalNav Outperforms Baselines and SOTA

We show a comparison of our feudal navigation agent to SOTA in Table II. We report success rate and SPL for FeudalNav, the version of our agent using the waypoint network with a single RGBD-Map input, and Stacked FeudalNav, which uses the waypoint network with three RGBD-Map inputs. Our method has shown a significant improvement in performance of 73% (straight) and 158% (curved) over all flat RL [53] baselines and 157% (straight) and 2341% (curved) over both behavior cloning (BC) methods [16] while using no RL, learning no metric map, and not training directly in a simulator.

On average, we achieve a 7% increase in performance on success rate over NRNS on the straight trajectories, despite not using odometry, not utilizing a graph, and only using $\sim 37k$ images for training (compared to the 3.5 million used by NRNS). Our SPL is consistently lower for straight trajectories because the hierarchical nature of our architecture prioritizes broader exploration [56] more than other methodologies, which is a desirable trait when finding objects in previously unseen environments. This is evidenced by our consistent improvement of 69% and 27% percent over NRNS on both success rate **and** SPL respectively for curved trajectories of all difficulty levels. In the real world, it is less likely that a robot will be tasked to find an object within a straight line of sight from itself. For this reason, performance on the curved trajectory case gives a more realistic prediction of real world performance.

VII. ABLATION STUDY

A. Different Network’s Effects on the Memory Proxy Map

We test the effectiveness of using multiple real world views as a contrastive learning augmentation. The ground truth distances between pairs of observations across a full trajectory

Path Type	MPM	WayNet	Worker	Easy		Medium		Hard		Average	
				Succ \uparrow	SPL \uparrow	Succ \uparrow	SPL \uparrow	Succ \uparrow	SPL \uparrow	Succ \uparrow	SPL \uparrow
Straight	\times	RGB	\checkmark	48.00	30.28	37.00	21.75	24.57	13.21	36.52	21.75
	\times	RGBD	\checkmark	48.20	31.70	39.40	21.50	24.94	12.99	37.51	22.06
	\times	3 RGBD	\checkmark	50.20	31.19	38.60	21.24	20.72	9.16	36.51	20.53
	\checkmark	RGBD-MPM (FeudalNav)	\checkmark	61.40	51.81	50.30	40.10	31.02	23.33	45.73	37.69
	\checkmark	3 RGBD-MPM (Stacked FeudalNav)	\checkmark	65.90	48.50	51.00	29.22	33.62	14.49	50.17	30.74
Curved	\times	RGB	\checkmark	34.70	11.20	32.60	13.02	18.20	7.24	28.5	10.49
	\times	RGBD	\checkmark	36.60	11.55	30.00	11.86	18.30	7.72	28.3	10.37
	\times	3 RGBD	\checkmark	39.50	11.91	32.80	11.75	15.70	5.65	29.33	9.77
	\checkmark	RGBD-MPM (FeudalNav)	\checkmark	41.30	19.51	32.60	17.10	18.60	10.88	30.83	15.83
	\checkmark	3 RGBD-MPM (Stacked FeudalNav)	\checkmark	56.40	21.37	44.10	17.41	21.00	7.30	40.50	15.36

TABLE III

WE CONDUCT AN ABLATION STUDY SHOWING THE EFFECT OF EACH MODULE IN FEUDALNAV ON OVERALL IMAGE-GOAL TASK PERFORMANCE. DESPITE SIMILAR SUCCESS RATE AND SPL, WE FIND A QUALITATIVE IMPROVEMENT AS WE ADD DEPTH AND 3 HISTORICAL FRAMES TO THE INPUT TO WAYNET. WE SEE LARGE PERFORMANCE IMPROVEMENTS AS WE ADD THE MEMORY PROXY MAP AS INPUT AS IT ALLOWS THE NETWORK TO HAVE A NOTION OF OBSERVATION FREQUENCY AND HELPS TO LOCALIZE THE AGENT IN THE ENVIRONMENT.

are compared to the distance between predicted image features for our high level manager network, which utilizes SMOG [51]. Moco [57], Resnet-18 [52], and Swav [58] are used as baselines for comparison. We compute inter-observation distance matrices in Figure 7 showing the ground truth and predicted feature MSE distances for a single trajectory from the human navigation dataset from the Copemish Gibson environment. In the figure, lower distances are darker/purple and higher distances are lighter/yellow. The more a latent space preserves geometric distances between image features, the more it should resemble the first square showing the distance matrix created using ground truth distances.

Swav [58] learns features that are highly diverse, as evidenced by the large distances between the features and the abundance of yellow in the graph. Resnet [52] has the reciprocal issue, where it learns highly similar features for all of the images in the trajectory, as evidenced by the large amount of purple in its graph. Both of these method’s features are unsuitable for navigation applications because they do not provide useful environment information. Moco [57] begins to mimic the GT distance matrix, but still mostly learns features that are similar to each other. SMOG [51] learns the most distance preserving latent space due to its ability to optimize inter-sample and inter-cluster distances simultaneously, making it the most useful for navigation purposes.

B. Full Hierarchy’s Affect on Image-Goal Task Performance

We also provide an ablation study to show how important each level of hierarchy is to our overall results in Table III. We incrementally add each piece of our architecture together and report the intermediary image-goal task results for the same experiment listed in Section V. The second column indicates whether or not the high level manager’s memory proxy map is included in the hierarchical navigation agent (\checkmark) or not (\times). The third column indicates what type of input WayNet takes in to make its navigation waypoint predictions. We provide results for a single RGB image, a single RGBD image, three sequential RGBD images, the combined input of an RGBD image and the MPM from the high level manager (FeudalNav), and the combined input of three RGBD images and three MPM’s (Stacked FeudalNav).

Despite their similar overall performance, we found that WayNet using RGB input performed qualitatively worse than using RGBD input because adding depth allowed the agent to avoid obstacles more efficiently. Again, we found that using three RGBD input images to WayNet also provided a qualitative performance boost to the agent as it stopped it from choosing to move in circles as it explored an environment. The added historical information imbued the agent with a notion of short term memory for recently visited locations that prompted it to explore new areas. We find a large improvement jump between using 3 RGBD images and a singular RGBD-Map input that is largely due to the introduction of memory into the navigation agent. The MPM 1) gives the agent information about the frequency of its historical and current locations and 2) helps localize the agent with respect to the image features of its historical locations. We also show that using a 3 RGBD-Map input provides another large improvement in success rate corresponding to adding extra memory to the system. However, these same gains cannot be seen in the SPL which indicates that this extra historical context may be pushing the agent to over prioritize exploration.

VIII. CONCLUSION AND DISCUSSION

Many visual navigation methods, as well as the one presented here, are developed in simulation environments. The issue of transferring from simulation to real environments in visual navigation is an important one. Recent work [9] has empirically evaluated the sim2real performance of visual navigation methods and concluded that *modular* approaches succeeded well, but end-to-end frameworks did not transfer well to real environments. Our approach falls into this modular learning designation that facilitates real world transfer.

With the ubiquity of advanced SLAM algorithms, the questions arise: If SLAM is solved, why learn?, why use visual navigation?, what is there to learn in navigation?; why not just build a metric map?”. These are important questions to address. First, SLAM is often computationally intensive and requires a considerable amount of development time and compute resources to manage. Each new environment requires development effort to manage the resulting large-scale optimization problem. Visual navigation holds the promise of

eventually being a light weight solution when no metric maps are built. But more importantly, visual navigation and learning-based navigation in general enables the system to learn about the dynamic environment that it is charged with navigating. The future challenges are learning nuances in navigating in social spaces such as: how close to other pedestrians, what speed, how to act in a crowd, and how to react to unexpected events. These nuances are location-specific, culture-specific and are learned and refined readily by navigating humans, but providing the same capability to robots remains largely unsolved.

REFERENCES

- [1] Edward C Tolman. Cognitive maps in rats and men. *Psychological review*, 55(4):189, 1948. 1
- [2] Elizabeth R Chrstil and William H Warren. From cognitive maps to cognitive graphs. *PloS one*, 9(11): e112544, 2014.
- [3] Michael Peer, Iva K Brunec, Nora S Newcombe, and Russell A Epstein. Structuring knowledge with cognitive maps and cognitive graphs. *Trends in cognitive sciences*, 25(1):37–54, 2021.
- [4] Russell A Epstein, Eva Zita Patai, Joshua B Julian, and Hugo J Spiers. The cognitive map in humans: spatial navigation and beyond. *Nature neuroscience*, 20(11): 1504–1513, 2017. 1
- [5] Nikolay Savinov, Alexey Dosovitskiy, and Vladlen Koltun. Semi-parametric topological memory for navigation. *arXiv preprint arXiv:1803.00653*, 2018. 1, 2
- [6] Devendra Singh Chaplot, Ruslan Salakhutdinov, Abhinav Gupta, and Saurabh Gupta. Neural topological slam for visual navigation. In *Proceedings of the IEEE/CVF Conference on Computer Vision and Pattern Recognition*, pages 12875–12884, 2020. 2
- [7] Piotr Mirowski, Matt Grimes, Mateusz Malinowski, Karl Moritz Hermann, Keith Anderson, Denis Teplyashin, Karen Simonyan, Andrew Zisserman, Raia Hadsell, et al. Learning to navigate in cities without a map. *Advances in neural information processing systems*, 31, 2018.
- [8] Kevin Chen, Juan Pablo de Vicente, Gabriel Sepulveda, Fei Xia, Alvaro Soto, Marynel Vazquez, and Silvio Savarese. A Behavioral Approach to Visual Navigation with Graph Localization Networks. In *Proceedings of Robotics: Science and Systems*, Freiburg/Breisgau, Germany, June 2019. doi: 10.15607/RSS.2019.XV.010.
- [9] Theophile Gervet, Soumith Chintala, Dhruv Batra, Jitendra Malik, and Devendra Singh Chaplot. Navigating to objects in the real world. *Science Robotics*, 8(79): eadf6991, 2023. 1, 8
- [10] Volodymyr Mnih, Koray Kavukcuoglu, David Silver, Andrei A Rusu, Joel Veness, Marc G Bellemare, Alex Graves, Martin Riedmiller, Andreas K Fidjeland, Georg Ostrovski, et al. Human-level control through deep reinforcement learning. *nature*, 518(7540):529–533, 2015. 1
- [11] Volodymyr Mnih, Koray Kavukcuoglu, David Silver, Alex Graves, Ioannis Antonoglou, Daan Wierstra, and Martin Riedmiller. Playing atari with deep reinforcement learning. *arXiv preprint arXiv:1312.5602*, 2013.
- [12] Timothy P Lillicrap, Jonathan J Hunt, Alexander Pritzel, Nicolas Heess, Tom Erez, Yuval Tassa, David Silver, and Daan Wierstra. Continuous control with deep reinforcement learning. *arXiv preprint arXiv:1509.02971*, 2015. 1
- [13] Dhruv Shah, Benjamin Eysenbach, Gregory Kahn, Nicholas Rhinehart, and Sergey Levine. Ving: Learning open-world navigation with visual goals. In *2021 IEEE International Conference on Robotics and Automation (ICRA)*, pages 13215–13222. IEEE, 2021. 1, 2
- [14] Ben Eysenbach, Russ R Salakhutdinov, and Sergey Levine. Search on the replay buffer: Bridging planning and reinforcement learning. *Advances in Neural Information Processing Systems*, 32, 2019. 1
- [15] Alexander Sasha Vezhnevets, Simon Osindero, Tom Schaul, Nicolas Heess, Max Jaderberg, David Silver, and Koray Kavukcuoglu. Feudal networks for hierarchical reinforcement learning. In *International Conference on Machine Learning*, pages 3540–3549. PMLR, 2017. 1, 2
- [16] Meera Hahn, Devendra Singh Chaplot, Shubham Tulsiani, Mustafa Mukadam, James M Rehg, and Abhinav Gupta. No rl, no simulation: Learning to navigate without navigating. *Advances in Neural Information Processing Systems*, 34:26661–26673, 2021. 1, 2, 6, 7
- [17] Fei Xia, Amir R. Zamir, Zhi-Yang He, Alexander Sax, Jitendra Malik, and Silvio Savarese. Gibson env: real-world perception for embodied agents. In *Computer Vision and Pattern Recognition (CVPR), 2018 IEEE Conference on*. IEEE, 2018. 2, 3, 6, 7
- [18] Manolis Savva, Abhishek Kadian, Oleksandr Maksymets, Yili Zhao, Erik Wijmans, Bhavana Jain, Julian Straub, Jia Liu, Vladlen Koltun, Jitendra Malik, Devi Parikh, and Dhruv Batra. Habitat: A Platform for Embodied AI Research. In *Proceedings of the IEEE/CVF International Conference on Computer Vision (ICCV)*, 2019. 2, 3
- [19] Angel Chang, Angela Dai, Thomas Funkhouser, Maciej Halber, Matthias Niessner, Manolis Savva, Shuran Song, Andy Zeng, and Yinda Zhang. Matterport3D: Learning from RGB-D Data in Indoor Environments. *International Conference on 3D Vision (3DV)*, 2017. 3
- [20] Saurabh Gupta, James Davidson, Sergey Levine, Rahul Sukthankar, and Jitendra Malik. Cognitive Mapping and Planning for Visual Navigation. In *Proceedings of the IEEE Conference on Computer Vision and Pattern Recognition (CVPR)*, July 2017. 2
- [21] Devendra Singh Chaplot, Dhiraj Gandhi, Saurabh Gupta, Abhinav Gupta, and Ruslan Salakhutdinov. Learning To Explore Using Active Neural SLAM. In *International Conference on Learning Representations*, 2019. 2
- [22] Alessandro Devo, Giacomo Mezzetti, Gabriele Costante, Mario L Fravolini, and Paolo Valigi. Towards generalization in target-driven visual navigation by using deep reinforcement learning. *IEEE Transactions on Robotics*, 36(5):1546–1561, 2020.
- [23] Zachary Seymour, Kowshik Thopalli, Niluthpol Mithun, Han-Pang Chiu, Supun Samarasekera, and Rakesh Kumar. Maast: Map attention with semantic transformers for efficient visual navigation. In *2021 IEEE International Conference on Robotics and Automation (ICRA)*, pages 13223–13230. IEEE, 2021. 2
- [24] Kevin Chen, Juan Pablo De Vicente, Gabriel Sepulveda, Fei Xia, Alvaro Soto, Marynel Vázquez, and Silvio

- Savarese. A behavioral approach to visual navigation with graph localization networks. *arXiv preprint arXiv:1903.00445*, 2019. 2
- [25] Dhruv Shah, Arjun Bhorkar, Hrish Leen, Ilya Kostrikov, Nick Rhinehart, and Sergey Levine. Offline reinforcement learning for visual navigation. *arXiv preprint arXiv:2212.08244*, 2022. 2
- [26] Yuhang He, Irving Fang, Yiming Li, Rushi Bhavesh Shah, and Chen Feng. Metric-Free Exploration for Topological Mapping by Task and Motion Imitation in Feature Space. *arXiv preprint arXiv:2303.09192*, 2023. 2
- [27] Dhruv Shah, Benjamin Eysenbach, Nicholas Rhinehart, and Sergey Levine. Rapid exploration for open-world navigation with latent goal models. *arXiv preprint arXiv:2104.05859*, 2021. 2
- [28] Nuri Kim, Obin Kwon, Hwiyeon Yoo, Yunho Choi, Jeongho Park, and Songhwai Oh. Topological Semantic Graph Memory for Image-Goal Navigation. In *Conference on Robot Learning*, pages 393–402. PMLR, 2023. 2, 6
- [29] Sacha Morin, Miguel Saavedra-Ruiz, and Liam Paull. One-4-All: Neural Potential Fields for Embodied Navigation. *arXiv preprint arXiv:2303.04011*, 2023. 2
- [30] Santhosh Kumar Ramakrishnan, Devendra Singh Chaplot, Ziad Al-Halah, Jitendra Malik, and Kristen Grauman. Poni: Potential functions for objectgoal navigation with interaction-free learning. In *Proceedings of the IEEE/CVF Conference on Computer Vision and Pattern Recognition*, pages 18890–18900, 2022. 2
- [31] Joao F Henriques and Andrea Vedaldi. Mapnet: An allocentric spatial memory for mapping environments. In *proceedings of the IEEE Conference on Computer Vision and Pattern Recognition*, pages 8476–8484, 2018. 2
- [32] Georgios Georgakis, Bernadette Bucher, Karl Schmeckpeper, Siddharth Singh, and Kostas Daniilidis. Learning to map for active semantic goal navigation. *arXiv preprint arXiv:2106.15648*, 2021. 2
- [33] Devendra Singh Chaplot, Dhiraj Prakashchand Gandhi, Abhinav Gupta, and Russ R Salakhutdinov. Object goal navigation using goal-oriented semantic exploration. *Advances in Neural Information Processing Systems*, 33: 4247–4258, 2020.
- [34] Ziad Al-Halah, Santhosh Kumar Ramakrishnan, and Kristen Grauman. Zero experience required: Plug & play modular transfer learning for semantic visual navigation. In *Proceedings of the IEEE/CVF Conference on Computer Vision and Pattern Recognition*, pages 17031–17041, 2022. 2, 6
- [35] Peter Dayan and Geoffrey E Hinton. Feudal reinforcement learning. *Advances in neural information processing systems*, 5, 1992. 2
- [36] Yuke Zhu, Roozbeh Mottaghi, Eric Kolve, Joseph J Lim, Abhinav Gupta, Li Fei-Fei, and Ali Farhadi. Target-driven visual navigation in indoor scenes using deep reinforcement learning. In *2017 IEEE international conference on robotics and automation (ICRA)*, pages 3357–3364. IEEE, 2017. 2
- [37] Ashish Kumar, Saurabh Gupta, David Fouhey, Sergey Levine, and Jitendra Malik. Visual memory for robust path following. *Advances in neural information processing systems*, 31, 2018. 2
- [38] Kuan Fang, Alexander Toshev, Li Fei-Fei, and Silvio Savarese. Scene memory transformer for embodied agents in long-horizon tasks. In *Proceedings of the IEEE/CVF conference on computer vision and pattern recognition*, pages 538–547, 2019.
- [39] Edward Beeching, Jilles Dibangoye, Olivier Simonin, and Christian Wolf. EgoMap: Projective mapping and structured egocentric memory for Deep RL. In *Joint European Conference on Machine Learning and Knowledge Discovery in Databases*, pages 525–540. Springer, 2020.
- [40] Lina Mezghan, Sainbayar Sukhbaatar, Thibaut Lavril, Oleksandr Maksymets, Dhruv Batra, Piotr Bojanowski, and Karteek Alahari. Memory-augmented reinforcement learning for image-goal navigation. In *2022 IEEE/RSJ International Conference on Intelligent Robots and Systems (IROS)*, pages 3316–3323. IEEE, 2022. 2
- [41] Scott Fujimoto and Shixiang Shane Gu. A minimalist approach to offline reinforcement learning. *Advances in neural information processing systems*, 34:20132–20145, 2021. 2
- [42] Hoang Le, Nan Jiang, Alekh Agarwal, Miroslav Dudík, Yisong Yue, and Hal Daumé III. Hierarchical imitation and reinforcement learning. In *International conference on machine learning*, pages 2917–2926. PMLR, 2018. 2
- [43] Alexander Vezhnevets, Yuhuai Wu, Maria Eckstein, Rémi Leblond, and Joel Z Leibo. Options as responses: Grounding behavioural hierarchies in multi-agent reinforcement learning. In *International Conference on Machine Learning*, pages 9733–9742. PMLR, 2020. 2
- [44] Valerie Chen, Abhinav Gupta, and Kenneth Marino. Ask your humans: Using human instructions to improve generalization in reinforcement learning. *arXiv preprint arXiv:2011.00517*, 2020. 2
- [45] Chengshu Li, Fei Xia, Roberto Martin-Martin, and Silvio Savarese. Hrl4in: Hierarchical reinforcement learning for interactive navigation with mobile manipulators. In *Conference on Robot Learning*, pages 603–616. PMLR, 2020. 2
- [46] Elliot Chane-Sane, Cordelia Schmid, and Ivan Laptev. Goal-conditioned reinforcement learning with imagined subgoals. In *International Conference on Machine Learning*, pages 1430–1440. PMLR, 2021. 2
- [47] Chengguang Xu, Christopher Amato, and Lawson LS Wong. Hierarchical robot navigation in novel environments using rough 2-d maps. *arXiv preprint arXiv:2106.03665*, 2021. 2
- [48] Jan Wöhlke, Felix Schmitt, and Herke van Hoof. Hierarchies of planning and reinforcement learning for robot navigation. In *2021 IEEE International Conference on Robotics and Automation (ICRA)*, pages 10682–10688.

IEEE, 2021. 2

- [49] Andrew Szot, Alex Clegg, Eric Undersander, Erik Wijmans, Yili Zhao, John Turner, Noah Maestre, Mustafa Mukadam, Devendra Chaplot, Oleksandr Maksymets, Aaron Gokaslan, Vladimir Vondrus, Sameer Dharur, Franziska Meier, Wojciech Galuba, Angel Chang, Zolt Kira, Vladlen Koltun, Jitendra Malik, Manolis Savva, and Dhruv Batra. Habitat 2.0: Training Home Assistants to Rearrange their Habitat. In *Advances in Neural Information Processing Systems (NeurIPS)*, 2021. 3
- [50] Paul-Edouard Sarlin, Daniel DeTone, Tomasz Malisiewicz, and Andrew Rabinovich. Superglue: Learning feature matching with graph neural networks. In *Proceedings of the IEEE/CVF conference on computer vision and pattern recognition*, pages 4938–4947, 2020. 4, 5, 6
- [51] Bo Pang, Yifan Zhang, Yaoyi Li, Jia Cai, and Cewu Lu. Unsupervised visual representation learning by synchronous momentum grouping. In *European Conference on Computer Vision*, pages 265–282. Springer, 2022. 4, 6, 7, 8
- [52] Kaiming He, Xiangyu Zhang, Shaoqing Ren, and Jian Sun. Deep residual learning for image recognition. In *Proceedings of the IEEE conference on computer vision and pattern recognition*, pages 770–778, 2016. 5, 8
- [53] Erik Wijmans, Abhishek Kadian, Ari Morcos, Stefan Lee, Irfan Essa, Devi Parikh, Manolis Savva, and Dhruv Batra. Dd-ppo: Learning near-perfect pointgoal navigators from 2.5 billion frames. *arXiv preprint arXiv:1911.00357*, 2019. 6, 7
- [54] Obin Kwon, Jeongho Park, and Songhwai Oh. Renderable Neural Radiance Map for Visual Navigation. In *Proceedings of the IEEE/CVF Conference on Computer Vision and Pattern Recognition*, pages 9099–9108, 2023. 6
- [55] Karmesh Yadav, Ram Ramrakhya, Arjun Majumdar, Vincent-Pierre Berges, Sachit Kuhar, Dhruv Batra, Alexei Baevski, and Oleksandr Maksymets. Offline visual representation learning for embodied navigation. *arXiv preprint arXiv:2204.13226*, 2022. 6
- [56] Ofir Nachum, Haoran Tang, Xingyu Lu, Shixiang Gu, Honglak Lee, and Sergey Levine. Why does hierarchy (sometimes) work so well in reinforcement learning? *arXiv preprint arXiv:1909.10618 (2019)*, 2019. 7
- [57] Kaiming He, Haoqi Fan, Yuxin Wu, Saining Xie, and Ross Girshick. Momentum contrast for unsupervised visual representation learning. In *Proceedings of the IEEE/CVF conference on computer vision and pattern recognition*, pages 9729–9738, 2020. 8
- [58] Mathilde Caron, Ishan Misra, Julien Mairal, Priya Goyal, Piotr Bojanowski, and Armand Joulin. Unsupervised learning of visual features by contrasting cluster assignments. *Advances in neural information processing systems*, 33:9912–9924, 2020. 8